Indoor Localization in Commercial 5G Environment with Single BS

Yue Dai[12], Liang Chen*[12], Xin Zhou[1],Yanlin Ruan[1], Ruizhi Chen [1]

[1] State Key Laboratory of Information Engineering in Surveying, Mapping and Remote Sensing
Wuhan University, Wuhan, China
[2] Hubei Luojia Laboratory, Wuhan, China
{daiyue2022, l.chen, x.zhou.whu, ruanyanlin, ruizhi.chen}@whu.edu.cn

Keywords: Fifth Generation (5G), Indoor Localization, Multibeam, Channel State Information (CSI), Reference Signal Received Power (RSRP).

Abstract

As commercial 5G systems rapidly expand, indoor positioning using 5G signals holds great potential for serving a large number of users. In this paper, an effective fingerprint solution is proposed for indoor positioning with 5G signal base station by exploring the multi-beam property. Multi-beam channel state information (CSI) and multi-beam reference signal received power (RSRP) are used as the observations for fingerprinting. To assess the effectiveness of the proposed scheme, field tests were conducted across various indoor environments. The results showed that the positioning accuracy is improved by more than 45% compared with the single beam by using the multi-beam characteristics of the 5G signal. Based on the multi-beam RSRP, the proposed scheme can achieve a positioning error of 67% below 1 meter. In the awareness of the two typical indoor deployments of 5G systems, i.e., the digital indoor distribution (DID) and the distributed antenna system (DAS), the paper also compared the 5G positioning performance in these two scenarios. The field tests showed that, the multi-beam in DID has more features than in DAS, which lead to a better positioning performance than that in DAS.

1. Introduction

With the rapid growth of urban areas, indoor positioning has become increasingly vital. It plays a crucial role in various indoor location-based services, including smart warehousing, precision marketing, and emergency safety systems (Chen et al., 2017). By 2027, the global market for these services is projected to reach US$57.24 billion, with an anticipated annual growth rate of 37.92% during the forecast period. Outdoors, in open spaces, the Global Navigation Satellite System (GNSS) provides precise location data, making it highly effective for outdoor location-based services (Shen et al., 2022). However, GNSS signals are blocked by barriers like concrete and are not well-received indoors, rendering them unsuitable for indoor positioning (Lu et al., 2020). Current indoor positioning technologies include ultra-wideband, Bluetooth, Wi-Fi, sound/ultrasound, pseudo-satellite, and geomagnetic methods (Ruan et al., 2022). Nevertheless, challenges like signal availability, complex spatial designs, and indoor signal transmission environments continue to hinder the development of accurate, reliable, and efficient indoor positioning solutions (Duan et al., 2020).

Currently, the large-scale deployment of fifth-generation (5G) mobile communication networks has introduced a range of new features, such as ultra-dense networks (UDN), antenna arrays, and advanced multiple access schemes. These innovations are designed to deliver high reliability, enhanced capacity, and low-latency positioning performance across broad areas. Moreover, these 5G technologies greatly support wireless positioning. According to the 3GPP Rel-18 protocol (3GPP, 2021), the aim of 5G New Radio (NR) indoor positioning is to achieve a horizontal absolute error of less than 10 meters and a vertical absolute error of less than 3 meters within a 95% confidence interval. To meet these requirements, significant research has been conducted in recent years on 5G NR-based positioning, which can be broadly categorized into geometric and fingerprint positioning methods.

Geometric positioning mainly encompasses techniques such as trilateration and triangulation, with key measurements including time of arrival (TOA), time difference of arrival (TDOA), observed TDOA (OTDOA), angle of arrival (AOA), and direction of arrival (DOA). For instance, Chen et al.(Chen et al., 2021) used the downlink synchronization signal block (SSB) from 5G NR to estimate TOA and proposed carrier phase ranging for indoor positioning. Similarly, Li et al.(Li et al., 2020) employed antenna arrays to estimate locations based on the joint AoA and flight time of uplink 5G signals. Zhang et al. (Zhang et al., 2023) utilized joint DoA/ToA from non-line-of-sight signals for positioning. However, geometric methods typically require multiple base stations, which is often difficult to achieve indoors, making implementation challenging in such environments.

On the other hand, fingerprint positioning relies on matching measurements from the test area to a pre-constructed database. This approach comprises two stages: the offline (training) stage and the online (testing) stage. During the offline phase, a fingerprint library is created using reference points, while in the online phase, the mobile device collects wireless signal characteristics and compares them with the database to estimate the location (Chen et al., 2013). Compared to geometric methods, fingerprinting has the advantage of not requiring multiple base stations or line-of-sight conditions, making it especially suitable for indoor environments. The measurements in fingerprinting primarily involve the received signal strength indicator (RSSI) and channel state information (CSI). A key observable of RSSI, the reference signal received power (RSRP), is often used in this approach. Meanwhile, CSI, which captures the

detailed signal propagation characteristics between transceivers, can also be applied for fingerprint recognition (Cho et al., 2010).

UE-side single gNB indoor positioning is an advanced research topic. While certain studies have demonstrated fairly good positioning accuracy, their application in commercial use is constrained by the high cost of receiving antenna arrays, particularly for standard smartphones.

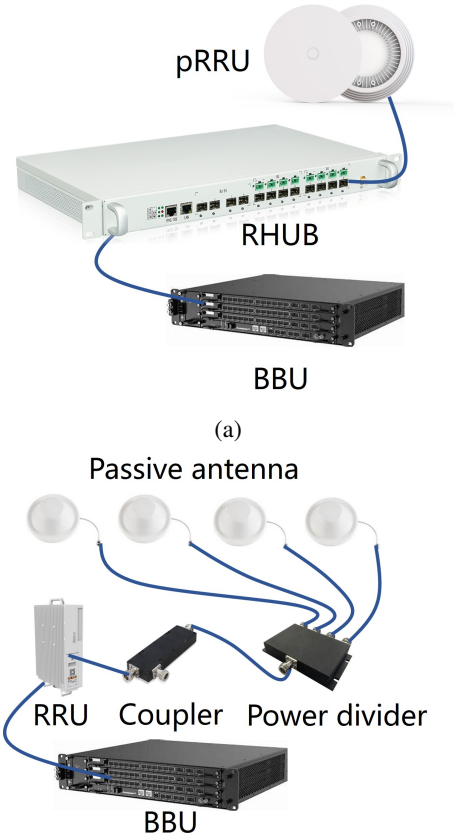

Figure 1. 5G Indoor Distribution System. (a) Digital Indoor Distribution (DID) (b) Distributed Antenna Systems (DAS).

To achieve UE-side positioning suitable for standard smartphones in a single gNB environment, we propose developing a fingerprint-based method using only one receiving antenna. In our previous work (Ruan et al., 2022), we introduced a fingerprint recognition approach based on channel state information (CSI) using a single-beam 5G signal and identified the fingerprint similarity issue. Specifically, certain fingerprints from different locations exhibit significant similarities, leading to increased positioning errors. As the commercial deployment of 5G accelerates, configurations have gradually evolved from single-beam non-standalone (NSA) networks to standalone (SA) networks. The 5G SA network introduces multi-beam technology to support high data transmission rates, enhancing both spectrum and energy efficiency. As illustrated in the figure, multi-beam transmits signals in multiple directions. Unlike single-beam networks, in a multi-beam 5G commercial environment, the UE can receive signals from different directions, improving the spatial distinguishability of various locations. However, the multi-beam shaping feature is currently limited to digital indoor distribution scenarios. Traditional indoor distribution systems (DAS) only support multi-beam features without the ability to implement shaping technology. Thus, we must account for two signal distribution states in current commercial 5G environments.

In this study, we applied multi-beam transmission technology, originally designed for communication, to positioning. Specifically, for two distinct commercial 5G deployment methods, we implemented 5G indoor positioning by constructing multi-beam CSI and RSRP fingerprint features. We also conducted field tests in various real indoor scenarios to verify the effectiveness of this approach.

2. 5G NR Feature Acquisition

2.1 5G NR Frame Structure

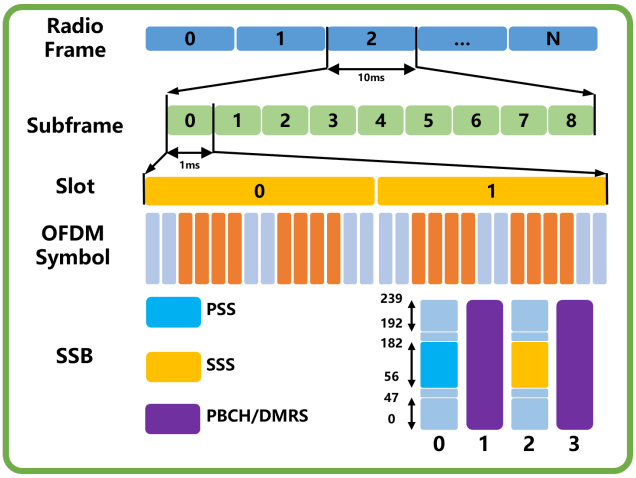

Figure 2. Time-frequency frame structure of the 5G NR signal.

The TS38.211 protocol specifies the standard frame structure for 5G signals. As illustrated in figure 2, 5G utilizes frames as the fundamental time unit, each lasting 10ms and containing 10 subframes, each of which is 1ms long. Each subframe is made up of multiple time slots, and within each time slot, there are 14 OFDM symbols.

In particular, as a system based on OFDM modulation to achieve robust propagation of signals in complex environments, the subcarrier spacing is a design parameter of the signal frame structure. The 5G signal itself supports multiple types of subcarrier spacing, which makes the number of time slots in a subframe unfixed. In the 5G frame structure, the smallest time unit is the OFDM symbol. A time slot contains a fixed number of OFDM symbols, and the subframe containing the time slot has a fixed time length. This makes the number of time slots in a subframe change when the subcarrier spacing changes. Among them, in the 5G standard, the supported subcarrier spacing $N_{SCS} = 15kHz \times 2^n$, (where $n \in \{0, 1, 2, 3, 4, 5, 6\}$). In particular, according to the TS38.300 protocol specification, if you want to support PBCH synchronization, the value range of n is $n \in \{0, 1, 3, 4, 5, 6\}$, and the subcarrier spacing is 15kHz, 30kHz, and 120kHz respectively. At present, the 5G working in my country works in the Sub-6 frequency band, and its subcarrier spacing includes 15kHz and 30kHz. The following mainly takes the 30kHz subcarrier spacing of the Sub-6 frequency band as the basis for analysis. The synchronization signal burst set of the 5G signal downlink contains multiple SSBs, which are

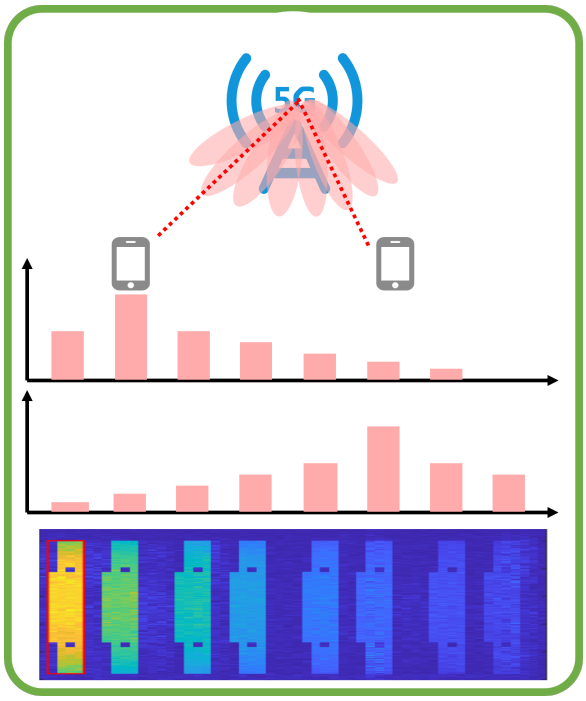

Figure 3. Diagram of multi-beam.

periodically transmitted at fixed intervals in one frame. According to TR 38.802, during the random access process, different SSBs use different antenna gains and phases to transform them into beamforming signals with different azimuths and elevations when transmitted through spatial channels. This makes different SSBs in the same frame have different spatial propagation characteristics. Therefore, 5G SSBs can use multi-beam fingerprints for positioning. The main use of SSB in communication is cell search and time synchronization. In terms of time, one SSB consists of four ODFM symbols. This consists of the primary synchronization signal (PSS), the secondary synchronization signal (SSS), and the physical broadcast channel (PBCH). Among them, PSS and SSS are used to estimate the start bit of the SSB frame and calculate the CID. The CID number N_{CID} is associated with the base station and is unique within a certain area to ensure that the UE is correctly synchronized and decoded. PBCH carries various information, including Master Information Block (MIB), DMRS symbols, etc. Among them, DMRS symbols are used for channel estimation.

The specific time-frequency relationship between PSS, SSS and PBCH is shown in the figure2. DMRS is located inside PBCH and has four frequency domain offsets $v = \{0, 1, 2, 3\}$ ($v = N_{CID} \bmod 4$).

2.2 5G NR signal demodulation

Demodulation for positioning mainly includes three steps, namely SSB detection, DMRS extraction and channel estimation

2.2.1 SSB detection According to the TS 38.211 protocol, 5G signals currently provide a total of 1008 candidate physical layer cell IDs, which are uniquely associated with base stations in a certain area and are used to manage the access between devices and base stations. The calculation of its number N_{CID} is:

$$N_{CID} = 3 \times N_{ID}^{1} + N_{ID}^{2} \tag{1}$$

Among them, $N_{ID}^{1} \in \{0, 1, 2, ..., 335\}$, $N_{ID}^{2} \in \{0, 1, 2\}$, are obtained by cross-correlation peak detection of the SSS reference signal and PSS reference signal generated in demodulation and the arrival signal received by the device. Among them, the reference signals used for cross-correlation are $d_{PSS}(n)$ and $d_{SSS}(n)$, which are uniquely related to N_{ID}^{2} and N_{ID}^{1}. The specific demodulation process is as follows.

PSS is a physical layer signal used to determine the frame boundary of the 5G signal. It is part of the m-sequence and functions as a specific linear feedback shift register. The PSS reference signal corresponds to $N_{ID}^{2} \in \{0, 1, 2\}$, with three variations in total. The received signal is frequency shifted at a fixed interval and then cross-correlated with different PSS reference signals in the time domain. By retrieving the peak value in the time-frequency cross-correlation, the corresponding coarse frequency deviation and the corresponding N_{ID}^{2} are obtained. After obtaining N_{ID}^{2}, we can obtain the PSS reference sequence of the current signal and its starting position. In 5G, SSB is sent once every two frames, which is located in one of the half frames. And the number of SSBs is related to the subcarrier type, signal frequency band, duplex working mode, etc. OFDM demodulate the synchronization waveform to extract the SSB resource block. Like PSS, SSS is an m-sequence and a physical layer signal that helps obtain the 5G signal frame boundary. The SSS reference signal corresponds to $N_{ID}^{2} \in \{0, 1, 2\}$ and $N_{ID}^{1} \in \{0, 1, 2, ..., 335\}$, with a total of 1008 types (the specific value of N_{ID}^{2} has been obtained through PSS decoding, and there are only 336 SSS reference signals that need to be constructed). For the SSB resource block that has been demodulated by OFDM, take out the SSS sequence and perform frequency domain cross-correlation with different SSS reference signals. By retrieving the peak value in the time-frequency cross-correlation, the corresponding N_{ID}^{1} is obtained. After completing PSS decoding and SSS decoding, the CID number N_{CID} of the current signal can be calculated using the formula 1.

2.2.2 DMRS extraction After calculating the CID, we need to search and demodulate the PBCH DMRS in the SSB. PBCH search is to construct a variety of different DMRS sequences and perform channel estimation and noise calculation with the current SSB. Among them, the DMRS index number with the largest signal-to-noise ratio is the beam number $\bar{i}_{SSB}$ corresponding to the current SSB. It also determines the least significant bit of the SSB resource block index required for PBCH scrambling initialization.First, calculate the position index of the DMRS in the SSB based on the CID number N_{CID} and generate the corresponding DMRS reference signal. Then, obtain the pilot signal for the received DMRS according to the demodulated SSB signal and beam number.

2.2.3 Channel estimation Due to different propagation environments, receivers at different locations often receive signals with different amplitudes and phases from the original signal. Through channel estimation, we can obtain the changing trend of the signal during propagation. The channel state is closely related to the environment in which the receiver is located, and shows strong spatial differences. This makes it possible to use the channel state as a spatial feature for indoor positioning research. Assume that the reference signal of the transmitter is X and the reference signal of the receiver is Y. Therefore, a standard model of signal propagation in the channel can be constructed:

$$Y = HX + N \tag{2}$$

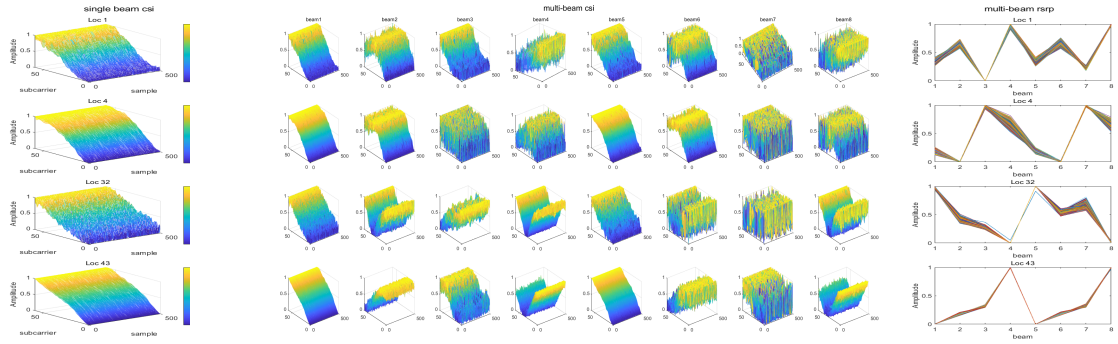

(a) (b) (c)

Figure 4. Comparison of the signal features of single beam vs. multi-beam transmitted from a gNB. (a) Positioning results with single beam at Locs 1, 4, 32, and 44, where CSI is similar. (b) CSI of multi-beam at Locs 1, 4, 32, and 44. (c) RSRP of multi-beam at Locs 1, 4, 32, and 44.

Where the channel is H and the noise in signal propagation is N. Using the least squares method to estimate the channel, we can get:

$$H = \left(X^H X\right)^{-1} \left(X^H Y\right) \tag{3}$$

Channel H is generally represented by Channel State Information (CSI).

Reference signal DMRS is a specific type of signal used for multiple purposes in 5G networks. They can be used for channel estimation, synchronization or other purposes. Reference signals are placed in specific resource elements. RSRP is a key indicator for evaluating network coverage. RSRP represents the received power of the synchronization signal reference signal. The calculation of RSRP is to obtain the reference SSS signal according to the CID, and the square of the mean of the conjugate multiplication of the received SSS signal and the reference SSS signal is the corresponding RSRP size. The specific expression is as follows:

$$RSRP = \lg |mean\left(\frac{d_{SSSRx}(n)}{d_{SSSRef}(n)}\right)|^2 \tag{4}$$

3. Method

3.1 Constructing dataset using multi-beam CSI

The dataset construction includes two steps: multi-beam CSI stacking and normalization.

3.1.1 Multi-beam CSI stacking For the hth sample at the pth position, the multi-beam CSI stacking is $\boldsymbol{b}_p^h = [\boldsymbol{c}_{1,p}^h, ..., \boldsymbol{c}_{l,p}^h, ..., \boldsymbol{c}_{L,p}^h] \in \mathbb{R}^{1\times(K\times L)}$. After superposition, the multi-beam CSI fingerprint of the pth position can be expressed as

$$\boldsymbol{C}_p = [\boldsymbol{b}_p^1, ..., \boldsymbol{b}_p^h, ..., \boldsymbol{b}_p^{N_s}]^T \in \mathbb{R}^{N_s\times(K\times L)} \tag{5}$$

After that, the total CSI fingerprint of the N_pth position in the test area can be further obtained, that is, $F = [\boldsymbol{C}_1, ..., \boldsymbol{C}_p, ..., \boldsymbol{C}_{N_P}]^T \in \mathbb{R}^{(N_P\times N_s)\times(K\times L)}$.

3.1.2 Normalization The CSI fingerprints of each beam have different orders of magnitude and need to be normalized to $[0, 1]$ through Min-Max normalization. At the pth position, the normalized CSI fingerprint can be written as

$$\boldsymbol{C}_p^{norm}(n) = \frac{\boldsymbol{C}_p(n) - \min(\boldsymbol{F})}{\max(\boldsymbol{F}) - \min(\boldsymbol{F})} \tag{6}$$

Where $\boldsymbol{C}_p(n)$ is the nth element of $\boldsymbol{C}_p$.

Taking the two-dimensional coordinates of the pth position $\boldsymbol{u}_p = (x_p, y_p)$ as the fingerprint label, the fingerprint dataset in the test area can be further obtained as

$$\Psi = \{(\boldsymbol{C}_1^{norm}, \boldsymbol{u}_1), ..., (\boldsymbol{C}_p^{norm}, \boldsymbol{u}_p), ..., (\boldsymbol{C}_{N_p}^{norm}, \boldsymbol{u}_{N_p})\} \tag{7}$$

3.2 Using multi-beam RSRP to build a dataset

Similar to using multi-beam CSI to build a dataset, the construction of a multi-beam RSRP dataset includes two steps: multi-beam RSRP stacking and normalization.

3.3 Position estimation using multi-beam features

To highlight the positioning performance of multi-beam, three classic machine learning (ML) algorithms are applied to position estimation: k-nearest neighbor (KNN), support vector machine (SVM), and tree of precision (TREE). These methods are widely used in positioning due to their simplicity and good performance in classification and regression tasks. Specifically, KNN is used to estimate the position by finding the nearest distance between online and offline features. SVM and TREE are used for positioning by learning the mapping relationship between features and positions. Position estimation is divided into offline and online stages.

4. Field test and performance analysis

To evaluate the positioning performance of multi-beam CSI and RSRP in 5G commercial environments, two distinct 5G signal deployment scenarios were chosen for experimentation: the conventional indoor DAS distribution mode and the digital indoor distribution mode. A test platform was constructed using software-defined radio, and the tests are detailed as follows.

4.1 Experimental platform

This paper develops a testing platform for signal sampling, recording, and demodulation based on SDR. The platform employs the USRP X310, a general-purpose software-defined radio peripheral, as the receiver and utilizes an atomic clock to provide a 10MHz reference clock input. The experiment captures 5G data using soft wireless devices and acquires location information via point layout. The figure illustrates a 5G signal sampling test setup.

According to the parameters of the 5G NR commercial base station (called gNB), the corresponding acquisition parameters in the SDR are adjusted to sample the 5G signal. The acquired 5G signal will be subjected to SSB detection, DMRS extraction and channel estimation according to the process of Section III-B to obtain CSI and RSRP information. In the experiment, the gNB parameters and transmission signals are defined by the 5G NR protocol TS 38.104 and selected by the operator China Mobile. According to the operator, the commercial signal corresponds to case C, operating in the n41 frequency band, with a subcarrier spacing of 30 kHz. The receiving end is configured with a 10 MHz bandwidth to capture the majority of the SSB signal power.

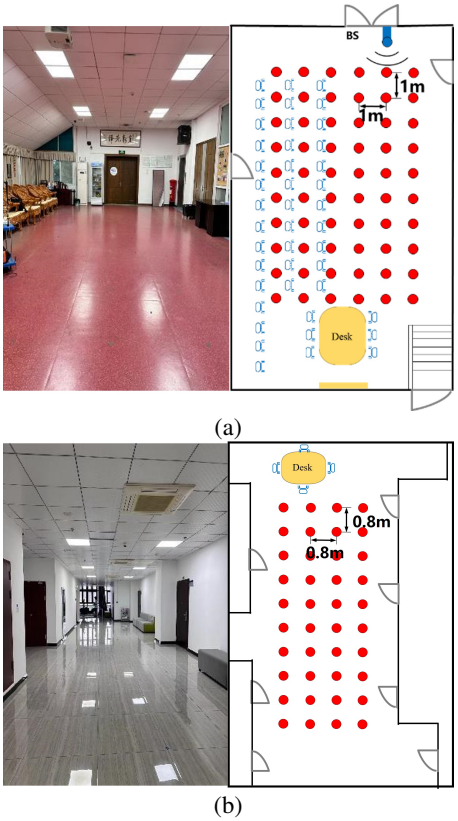

Figure 5. Experimental scenarios.
(a) DID scenario. (b) DAS scenario.

4.2 Experimental scenarios

Scenario 1 takes place in a meeting room on the fourth floor of the LIESMARS building, furnished with numerous chairs, desks, and a podium. In this setting, a 5G system is deployed using a digital indoor distribution model, with only one base station (BS) clearly detectable. Figure 5(a) illustrates the test environment, where 60 test points are arranged. The two-dimensional coordinates of the BS are preset at (0 m, 0 m), while the coordinates of position 01 are set at (2 m, 1.5 m). The grid spacing is 1.0 m. Measurements from the commercial 5G BS were collected for 10 seconds at each grid point to build the training database, followed by another 10 seconds for testing. After the procedure outlined in Section 2, 500 samples were obtained for training, and an additional 500 samples were used for testing.

Scenario 2 takes place in a typical office corridor, where the 5G system is deployed as a DAS by China Mobile, the commercial operator. Only one 5G base station (BS) is detectable in this scenario. A passive signal amplification antenna is installed behind the ceiling, resulting in non-line-of-sight (NLOS) transmission. The layout of the test scenario is illustrated in Figure 5(b), with 40 preset test points in this area. The coordinates of position 01 are set at (0, 0), and the distance between each grid is 0.8 meters. Similar to the tests conducted in the meeting room, measurements are taken over 10 seconds in each grid, yielding 500 samples for training. Subsequently, an additional 10 seconds of measurements are collected for testing.

4.3 Experimental results

In order to clearly compare the positioning performance in different algorithms, the cumulative distribution function (CDF), mean absolute error (MAE) and root mean square error (RMSE) are used as statistical indicators. Table 1 summarizes the positioning results. It can be clearly seen from the table that in the case of single-beam positioning, the MAE errors of KNN, SVM and TREE in scenario 1 are 0.74m, 0.66m and 1.25m respectively. For multi-beam positioning, the corresponding errors are 0m, 0.01m and 0.37m, i.e., a reduction of 100%, 98.5% and 71.4% respectively. Similarly, in scenario 2, the MAE errors of KNN, SVM and TREE are all reduced by more than 51% when using multi-beam compared to using single beam. By compar-

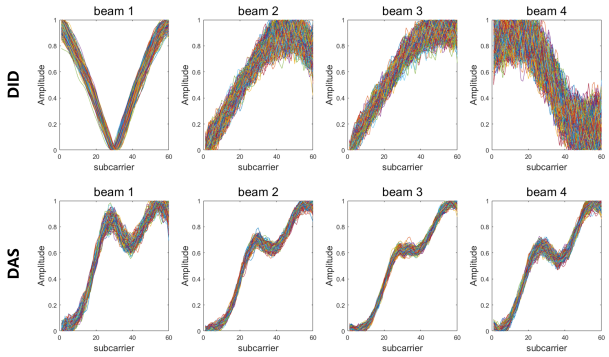

Figure 6. Multi-beam CSI feature comparison - DID and DAS.

ison of the positioning performance in DAS and DID, both system has shown the characteristic of multi-beam transmission. However, since the DAS system can not support beamforming technology effectively, it only distinguishes different beams by adjusting the signal strength of each SSB. Therefore, the characteristics in the multi-beam is not as obvious as in DAS. As can be seen from figure 6, in the DID system, the CSI between multiple beams have independent features, but in the DAS system, the CSI between different beams are relatively similar. Thus, it is reasonable that, the positioning accuarcy in DID is better than in DAS, as shown in Table 1.

Table 1. Statistics of different performance metrics in multi-beam and single beam positioning

Scenario	Algorithm	Beam type	67% error (m)	95% error (m)	MAE (m)	RMSE (m)
DID office	KNN	Single beam CSI	0.00	5.09	0.74	1.85
		Multi-beam CSI	**0.00**	**0.00**	**0.00**	**0.00**
		Multi-beam RSRP	**0.00**	**0.00**	**0.03**	**0.31**
	SVM	Single beam CSI	0.00	5.38	0.646	1.72
		Multi-beam CSI	**0.00**	**0.00**	**0.01**	**0.26**
		Multi-beam RSRP	**0.00**	**4.24**	**0.92**	**1.79**
	TREE	Single beam CSI	0.71	5.65	1.25	2.44
		Multi-beam CSI	**0.00**	**0.94**	**0.37**	**1.26**
		Multi-beam RSRP	**0.00**	**0.95**	**0.42**	**1.32**
DAS office	KNN	Single beam	0.00	1.00	0.13	0.70
		Multi-beam CSI	**0.00**	**0.00**	**0.01**	**0.08**
		Multi-beam RSRP	**0.00**	**0.00**	**0.09**	**0.49**
	SVM	Single beam CSI	0.00	2.24	0.23	0.82
		Multi-beam CSI	**0.00**	**1.40**	**0.19**	**0.76**
		Multi-beam RSRP	**0.00**	**2.00**	**0.19**	**0.81**
	TREE	Single beam CSI	0.00	2.23	0.33	1.03
		Multi-beam CSI	**0.00**	**1.40**	**0.21**	**0.93**
		Multi-beam RSRP	**0.00**	**1.41**	**0.18**	**0.79**

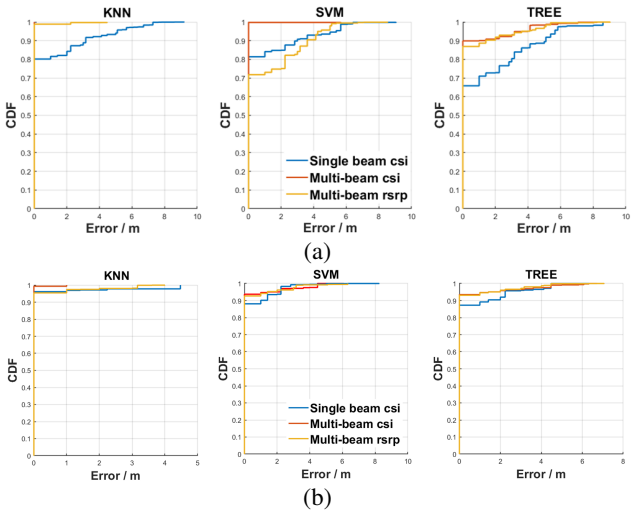

Figure 7. CDF of positioning errors with multi-beam and single beam in different scenarios. (a) DID scenario. (b) DAS scenario.

Figure 7 shows the CDF of multi-beam and single-beam positioning errors. The figure clearly shows that multi-beam performs significantly better than single-beam in all test scenarios implemented by the ML algorithms.

Therefore, multi-beam can effectively solve the CSI similarity problem and improve 5G indoor positioning accuracy by enhancing the spatial discrimination of signals.

5. Conclusion

This study addresses the challenge of indoor positioning in various 5G deployment scenarios. By analyzing the spatial distribution of signals, we find that multi-beam technology increases signal diversity and enhances spatial differentiation between locations. Therefore, the multi-beam characteristics are utilized for positioning, using both multi-beam CSI and multi-beam RSRP fingerprint recognition methods. To evaluate the effectiveness of the proposed approach, we apply three classical machine learning algorithms during the positioning estimation phase and test them in real-world conditions across two distinct 5G deployment scenarios. The test results show that MASE positioning within 1.3 m is achieved by taking advantage of the multi-beam. Compared with a single beam, the accuracy is improved by more than 20%. This shows that introducing multi-beam technology into commercial 5G indoor positioning is a feasible solution. Future research will focus on algorithm optimization to achieve a balance between multi-beam positioning performance and computational cost.

Acknowledgment

This work was supported in part by the National Natural Science Foundation of China under Grant 42171417, in part by the Medium- and Long-term Scientific and Technological Planning Projects for Radio, Television and Audio-Visual Networks , in part by the Special Fund of Hubei Luojia Laboratory under Grant 220100008, and in part by the Guangxi Science and Technology Major Project under Grant AA22068072.

References

3GPP, 2021. 3GPP TS 22.261 version 18.13.0 Release 18 - service requirements for cyberphysical control applications in vertical domains. 3GPP Working Group Report.

Chen, L., Pei, L., Kuusniemi, H., Chen, Y., Kröger, T., Chen, R., 2013. Bayesian fusion for indoor positioning using bluetooth fingerprints. *Wireless personal communications*, 70, 1735–1745.

Chen, L., Thombre, S., Järvinen, K., Lohan, E. S., Alén-Savikko, A., Leppäkoski, H., Bhuiyan, M. Z. H., Bu-Pasha, S., Ferrara, G. N., Honkala, S. et al., 2017. Robustness, security and privacy in location-based services for future IoT: A survey. *Ieee Access*, 5, 8956–8977.

Chen, L., Zhou, X., Chen, F., Yang, L.-L., Chen, R., 2021. Carrier phase ranging for indoor positioning with 5G NR signals. *IEEE Internet of Things Journal*, 9(13), 10908–10919.

Cho, Y. S., Kim, J., Yang, W. Y., Kang, C. G., 2010. *MIMO-OFDM wireless communications with MATLAB*. John Wiley & Sons.

Duan, Y., Lam, K.-Y., Lee, V. C., Nie, W., Li, H., Ng, J. K.-Y., 2020. Packet delivery ratio fingerprinting: Toward device-invariant passive indoor localization. *IEEE Internet of Things Journal*, 7(4), 2877–2889.

Li, Y., Zhang, Z., Wu, L., Dang, J., Liu, P., 2020. 5g communication signal based localization with a single base station. *2020 IEEE 92nd Vehicular Technology Conference (VTC2020-Fall)*, IEEE, 1–5.

Lu, X., Chen, L., Shen, N., Wang, L., Jiao, Z., Chen, R., 2020. Decoding PPP corrections from BDS B2b signals using a software-defined receiver: An initial performance evaluation. *IEEE sensors journal*, 21(6), 7871–7883.

Ruan, Y., Chen, L., Zhou, X., Guo, G., Chen, R., 2022. Hi-Loc: Hybrid indoor localization via enhanced 5G NR CSI. *IEEE Transactions on Instrumentation and Measurement*, 71, 1–15.

Shen, N., Chen, L., Lu, X., Ruan, Y., Hu, H., Zhang, Z., Wang, L., Chen, R., 2022. Interactive multiple-model vertical vibration detection of structures based on high-frequency GNSS observations. *GPS Solutions*, 26(2), 48.

Zhang, Y., Liu, Y., Liu, Y., Wu, L., Zhang, Z., Dang, J., 2023. Multi-ris-assisted millimeter wave single base station localization. *2023 4th Information Communication Technologies Conference (ICTC)*, IEEE, 115–120.